Sensors and Actuators B 238 (2017) 532–539

Contents lists available at ScienceDirect

Sensors and Actuators B: Chemical

journal homepage: www.elsevier.com/locate/snb

An image-driven drop-on-demand system

Camille Girabawe, Seth Fraden*

Department of Physics, Brandeis University, 415 South Street, Waltham, MA 02453, USA

ARTICLE INFO

Article history:
Received 7 June 2016
Received in revised form 10 July 2016
Accepted 14 July 2016
Available online 18 July 2016

Keywords:
Pneumatic valve
Feedback loop
Image analysis
Osmosis
Mass transport

ABSTRACT

This paper introduces a microfluidic system whose purpose is to precisely and quantitatively characterize and control the mass transport between aqueous drops in a continuous oil background. The system consists of an image-based drop-on-demand microfluidic device based on programmable PDMS pneumatic valves. It consists of a closed feedback loop that uses real time image analysis to measure and generate a pre-set number of droplets one at a time with prescribed volume and composition in a specified sequence. Drops generated on-chip are exported off-chip into glass capillaries. In addition, the system allows the control of the spacing distance between adjacent drops, which is a key parameter regulating the rate of material transport between drops. Three studies illustrating the versatility of the device are presented: (1) Synchronization of chemical oscillations in networks of droplets containing the Belousov–Zhabotinsky reaction as a function of differences in drop volume. (2) Studies of the nucleation and stability of metastable amorphous calcium carbonate as a function of the spacing and composition of reacting drops. (3) Measurements of the exchange of water between drops immersed in oil as a function of added surfactant to address the question of whether micelles facilitate transport of salt between drops.

1. Introduction

The use of droplet-based microfluidics in which small quantities of reagents are precisely compartmentalized to create multitudes of individual reactors has proven useful in biological and chemical studies [1–8]. Droplets are generated by using flow to create interfaces between two immiscible solutions, such as water in oil, that are stabilized by addition of surfactant molecules [9–11]. Flow-focusing is a popular method in which a continuous aqueous phase is injected in a continuously flowing oil phase. The size of drops is dictated by the nozzle size and ratio between flow rates of the two phases, and the method is capable of generating identical droplets at rates up to 10 kHz. However, such high frequency drop generation techniques lack the freedom to arbitrarily control the size of specific drops and control the distance between adjacent drops [8,9,12]. It is also impossible to control the exact number of drops to be generated. As an alternative, drop-on-demand (DOD) techniques were introduced in order to make one drop at a time [13–16]. Our system falls into the category of DOD devices that operate by generating aqueous droplets through controlling the amplitude and duration of pressure pulses in the aqueous phase using a PDMS chip with an off-chip solenoid [14], or piezoelectric valve [16]. Similarly to high throughput drop makers, these DOD systems are most often operated in a mode in which the oil phase flows continuously, which is in contrast to our system. Moreover, our system is able to control positions of multiple drops in a linear array inside a glass capillary tube in contrast to the recently emerging technique of inkjet printing that controls the positions of drops on an open surface [17,18].

Here, we introduce a closed-loop image based drop-on-demand system that offers the ability to produce a specific number of aqueous droplets with prescribed volumes, ordered in a desired sequence by size or composition and with a controllable distance between adjacent droplets. The purpose of this system is to precisely and quantitatively characterize and control the mass transport between aqueous drops in a continuous oil background. The basic concept of our DOD device, illustrated in Fig. 1, is that aqueous droplets are generated in two steps in a cross-flow (T-junction) geometry in which an aqueous line intersects an oil line at right angles. First, an on-chip PDMS pneumatic valve is opened on the pressurized aqueous line while the oil inlet is closed. This causes water to flow as long as the aqueous valve is opened. We employ a sequence of brief valve openings which cause the water volume to increase in discrete steps, forming a *plug* of water that extends

* Corresponding author.
E-mail address: fraden@brandeis.edu (S. Fraden).

http://dx.doi.org/10.1016/j.snb.2016.07.065
0925-4005/

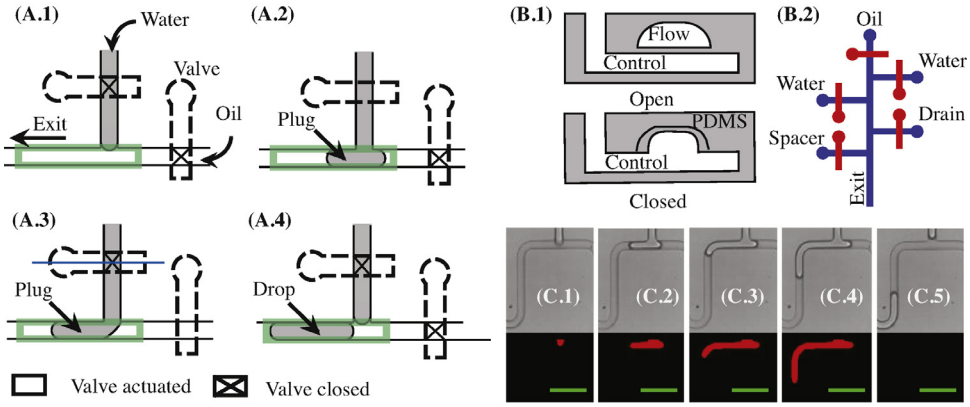

Fig. 1. (A) Schematic steps to generate a drop in a T junction: After selecting the region of interest (ROI), shown as a green rectangle, captured images are sequentially binarized in real-time to measure the plug area, corresponding to the area of water in the ROI. (A.1) Both water and oil inlets are closed, (A.2) the water inlet is opened repetitively while the oil is held closed, (A.3) when the preset drop size is reached, the water valve is closed and the oil valve is opened to shear the plug and form (A.4) a drop. (B.1) Schematics of side views of open and closed valves. (B.2) Schematic of the chip with flow channels in red and control channels in blue. (C) Sequence of images being processed in real-time. Top row: photographs showing the elongation of a plug of aqueous phase that extends into the oil channel. Bottom row: the corresponding binarized images where red is the plug area. In (C.5) No object is detected because the drop has exited the ROI. Green scale bars in each photograph are 200 μm long. (For interpretation of the references to colour in this figure legend, the reader is referred to the web version of this article.)

into the oil channel. Simultaneously the water volume is measured using real-time image processing. When the pre-set target size is reached, the oil valve is momentarily opened, which shears off the aqueous plug and forms a drop. Similarly, the separation distance between adjacent drops is controlled using two additional channels, the *drain channel*, filled with oil and connected to a negative pressure source to remove oil between drops and the *spacer channel*, filled with oil and connected to a positive pressure source to add oil between drops.

PDMS is highly permeable to gas and apolar chemical species. Therefore, to study mass transport between drops in oil we transfer the drops off-chip to a cylindrical glass capillary, which is impermeable to all chemicals. This ensures that chemicals only exchange between drops and do not leak out into the microfluidic device. We note that inter-drop distance is an unexplored variable in mass transport experiments involving microfluidic emulsions. This system allows control of the drop spacing, both on-chip and off-chip in the glass capillaries. In this paper, we characterize the system and present three experiments that demonstrate the benefits of being able to control the size and composition of a few drops, as well as the distance between adjacent drops. These particular experiments, chosen to illustrate the versatility of the drop-on-demand technique, were (1), studies of synchronization of chemical oscillations between adjacent drops of different volume, but with the same chemical composition of the Belousov–Zhabotinsky reaction mixture [3], (2) studies of the nucleation and stability of the metastable amorphous calcium carbonate (ACC) phase in which adjacent drops contain different volatile chemicals and have different inter-drop spacing, and (3) studies of the effect of surfactant on the transport of water between droplets containing different concentrations of sodium chloride as a function of inter-drop spacing.

2. Methods and experimental setup

The drop-on-demand system is comprised of four main functional units, which together function as a closed feedback loop using real-time image analysis to control the size of each drop, consisting of (1) the PDMS chip, (2) external pressure and valve controllers operated by LabVIEW, (3) a microscope and video camera and (4) a cylindrical glass capillary.

2.1. PDMS chip and glass capillary

Using standard photolithography methods [13], a PDMS chip was fabricated with two independent water inlet channels forming a T junction with a third oil inlet. Towards the outlet, the chip has two addition channels, the “spacer” and the “drain” used respectively to add or remove oil between two drops positioned on opposite sides of its nozzle. A schematic of the chip is shown in Fig. 1B.2. The chip has one push-up pneumatic valve (drawn in red) on each flow channel (drawn in blue) which enables the corresponding fluid to flow when actuated [13]. The chip is made of two PDMS layers, the top layer containing the flow channels and the bottom layer containing the control channels. There is a 20 μm PDMS membrane between the two layers that acts as the valve. In order to close the flow channel, pressure is applied to the corresponding control channel which has an inlet but no outlet. Since the PDMS is elastic, the thin membrane between the two layers stretches and fills the flow channel. When the pressure is released, the membrane relaxes thereby opening the valve as shown in Fig. 1A and B. The design CAD files and detailed manufacturing instructions are provided in Appendix A and B. At the exit channel of the PDMS chip, a cylindrical capillary (VitroCom) of 100 μm inner diameter pretreated with (tridecafluoro-1,1,2,2-tetrahydrooctyl) trichlorosilane to maintain hydrophobicity, is connected in order to collect and store drops. The treatment of the capillaries consists in coating the capillary surface with silane vapor by enclosing capillaries with 10 pl of silane inside a vacuum flask for 12 h at −5 Psi. Once drops are collected, the capillary was sealed and clamped to a microscope slide with epoxy.

2.2. Pressure and valve control hardware

The pressure and valve controller hardware includes proportional valves KPI-VP3-05-09-25 purchased from Kelly Pneumatic Inc. which are used as pressure regulators. These proportional valves establish a user programmable constant pressure in 2 ml vials containing either reagents or oil which are connected to the chip using polytetrafluoroethylene (PTFE) capillary tubes. The vials are sealed with caps in which two holes were drilled. One hole held tubing filled with compressed air that connected the vial to the proportional valve. The other hole held tubing immersed in the fluid contents of the vial and connected the vial to the inlets of the PDMS

chip. The hardware also includes solenoid valves LHDA052311H and solenoid manifold LFMX0510533BF both purchased from the Lee Company. A normally open solenoid manifold was chosen such that with a zero voltage applied to solenoid valves, the control channel of the PDMS is pressurized thereby closing the on-chip pneumatic valve. Due to the compressibility of air and its permeation through the PDMS [19], the tubes connected to the control channels were filled with water in order to improve valve performance.

2.3. The software

The Drop-on-Demand system includes a Nikon microscope with a Marlin CCD camera (Allied Vision Technologies GmbH), to capture images of the drop generation events and import them to LabVIEW for analysis as described in Fig. 1C. This program analysed images, captured at a frame rate of 30 frames per second and in real-time used edge detection and object filling algorithms to find and measure the area of a plug of water. Because the height of the channels is known, the volume of the plug can be deduced from the area. Once the volume of the plug reaches the desired volume, LabVIEW actuates the electronic circuit which drives the hardware pressure and valves controllers in such a way as to sever the plug and create a drop. A similar method is used to set the separation distance between adjacent drops. Two drops are positioned on opposite sides of the drain and the spacer channels which contain oil. Pneumatic valves on the drain and spacer channels are alternatively actuated in consecutive brief valve openings to remove or add oil between the drops of interest until a pre-set distance is achieved. The separation distance is measured through image analysis. Drop separation distance was accurately controlled for drops inside the rectangular channel of the PDMS chip. The separation distance was found vary as an affine function after the drops were exported to an external cylindrical glass capillary due to a change in channel cross-section at the junction of the rectangular PDMS channel and cylindrical glass capillary.

The system hardware and software were designed such that one platform can control a maximum of eight modules [20]. A module is defined as an ensemble of one pressure controller and one solenoid valve to drive one inlet/outlet channel.

3. Working mechanism and characterization

This section describes the operating details and characterization of the Drop-on-Demand instrument. To test the system, water in oil drops were produced using surfactant [21] (RAN Biotechnologies FluoroSurfactant) stabilized oil (3M™ Novec™ 7500 Engineered Fluid). Generating a drop begins with pre-setting the target size. Then, with the oil inlet channel held closed by the push-up valve, the solenoid valve controlling the water inlet is repetitively actuated, as illustrated in Fig. 1. In Fig. 1A.1, the aqueous phase is introduced from the top. In Fig. 1A.2 and C.1-3, after a few pressure pulses, the size of the aqueous plug has increased. Each single pressure pulse generates an increase in the size of the water plug, whose area is measured via the LabView program in real time. When the target size is reached (Fig. 1A.3 and C.4), the water inlet channel is closed and a pulse of pressure is applied to the oil channel to sever the aqueous plug from the inlet channel and create an isolated drop (see Fig. 1A.4 and C.5). We observed severing occurs at the junction of the oil and water channels as illustrated in Fig. 1A.1. Therefore, the software estimates the volume of the drop to be formed as the product of the area bounded by the detected edges of the channel and the height of the channel. The software can be programmed to automatically generate a sequence of a pre-set discrete number of drops with prescribed sizes. Using a chip with two aqueous

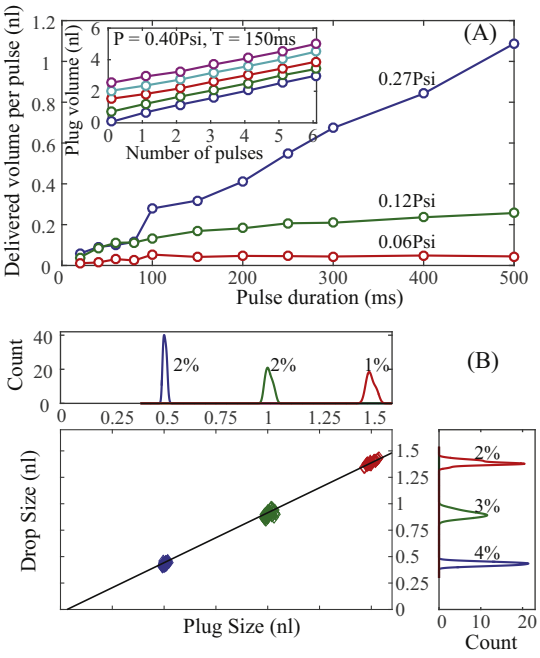

Fig 2. Characterization of the system (A) Volume delivered per pulse as a function of pulse duration and pressure. Each data point corresponds to the slope of the plug volume as function of the number of pulses as shown in the inset. Arbitrary offsets in volume were introduced to make the inset readable. (B) Linear relationship between final drop size and plug size. Along the top and right margins, the plug and drop size distributions are plotted with their relative standard deviations.

inlet channels it is also possible to generate two different types of droplets precisely ordered by chemical contents, concentration or size. Moreover, with two additional oil channels it is also possible to control the distance between two consecutive droplets. The "spacer" channel is filled with oil at a positive pressure and is used to inject oil so as to increase the separation between two drops located on opposite sides of the spacer nozzle. Similarly, applying a negative pressure on the "drain" channel, it is possible to remove oil between two drops hence reducing their separation. As it was done to control the size of the drop, the system can be programmed to set a desired distance between adjacent drop as shown in video2 in Appendix G.

In order to characterize the system, drops with a specific target size and specific separation distance were generated and measured. Results of these measurements are shown in Fig. 2. The volume of the water plug was found to grow linearly with the number of pulses at constant pressure and pulse duration (Fig. 2A inset). The volume delivered per pulse was found to be non-linear for small pulse duration (Fig. 2A). We speculate this is due to PDMS compliance. When the PDMS is pressurized, the channel is strained. Opening the valve allows the PDMS to contract which creates flow in addition to pressure driven flow. Consequently, within this non-linear regime, it is possible to generate a change in size of the meniscus as small as 20 pl using a pulse duration of 20 ms and 0.06 Psi. However, at this extremely low pressure, but with a longer pulse duration of 500 ms, it was found that the volume of water plug did not change beyond 20 pl. In other words, at this low pressure, when the valve was opened there was no flow of water, but only a 20 pl spurt. We speculate that the spurt is caused by the relaxation of the strained PDMS and then the Laplace pressure of the oil-water interface exceeds the external pressure of 0.06 Psi, thereby stopping the flow. This non-linear behaviour persists until the pressure is raised above 0.12 Psi. Above 0.12 Psi and pulse durations longer than 80 ms with 0.27 Psi applied on the oil inlet, the final drop size was found to grow linearly with respect to the size

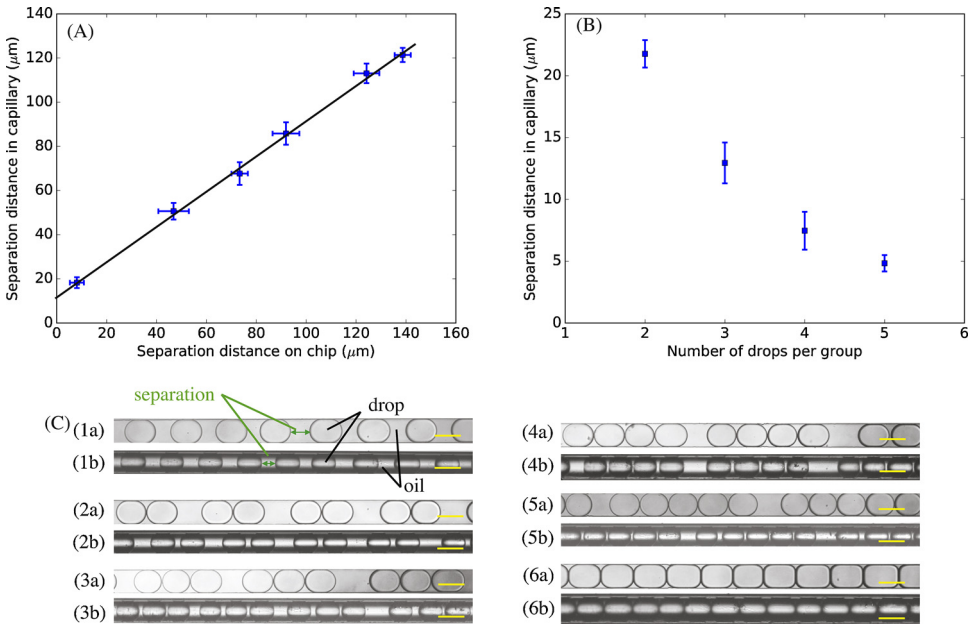

Fig 3. Characterization of separation distance between drops on- and off-chip. (A) The separation distance between drops exported to a cylindrical glass capillary as a function of the separation distance measured on chip (B) Separation of exported drops as a function of number of drops for drops that were initially touching while on chip. (C) Series of photographs of drops on PDMS chip (top, a) and after exported to glass capillaries (bottom, b) as a function of number of drops in a group. Group size one (1), two (2), three (3), four (4), five (5) and all drops (6). Yellow scale bars in each photograph are 120 μm long. (For interpretation of the references to colour in this figure legend, the reader is referred to the web version of this article.)

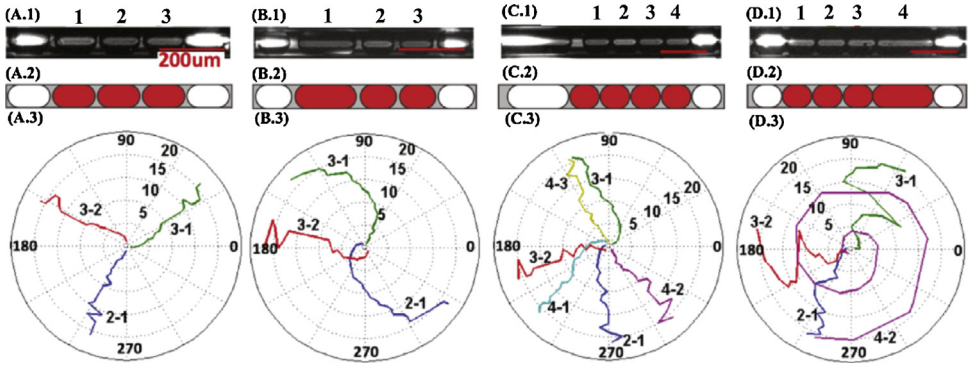

Fig 4. Groups of (A) three and (C) four BZ drops with same size, (B) three and (D) four BZ drops with different size bounded by two drops in which the reaction was supressed using blue light. For each group, (.1) schematic illustrating lighted boundary BZ drops (white sphero-cylinders), active BZ drops (red) and the oil (grey) between drops in a cylindrical glass capillary, (.2) images from raw experiment and (.3) phase difference (polar angle in units of degree) vs. time (radial in units of oscillation period). Pairs of drops with the same size (A and C) synchronize by locking at some constant phase difference while those pairs composed of drops of different size (B and D) do not synchronize. (For interpretation of the references to colour in this figure legend, the reader is referred to the web version of this article.)

of plug from which it was formed (Fig. 2B). For the three investigated drop sizes, 0.43 nl, 0.90 nl and 1.4 nl the standard deviation was found to be 0.02 nl, 0.03 nl and 0.03 nl respectively, equivalent to relative errors of 4%, 3% and 2%. The non-linear dependence of drop volume on pressure could be avoided by using a microfluidic device composed of a material with greater rigidity than PDMS, such as a thermoplastic like cyclic olefin copolymer [22].

Results of the experiments carried out to characterize the separation distance between adjacent drops on- and off-chip are presented in Fig. 3. After drops were generated inside rectangular channels on the PDMS chip they were exported to a cylindrical capillary inserted at the exit of the outlet channel. Rapid export of the drops from the PDMS to glass capillaries produced an uncontrollable and large separation between drops. However, slow exportation, achieved using a low, constant pressure of 0.13 Psi in the oil phase, produced a controllable separation distance. The separation distance between drops exported to the cylindrical capillary as a function of their initial separation distance while they were inside the rectangular channel on-chip is an affine function with a Pearson correlation coefficient of 0.999, as shown in Fig. 3A. A series of experiments designed to characterize how drop separation varied on- and off-chip were performed in which drops were exported in groups of 1–5 and a full capillary of close-packed drops (see Fig. 3C). The constant offset in the separation distance shown in Fig. 3A was found to be a monotonic decreasing function of the number of drops in a group, as illustrated in Fig. 3B, with the separation approaching zero as the number of drops per group increased.

We anticipate several limitations to this system. The current method is not advised for handling volatile materials which can corrode the pneumatic valves. Also, viscous fluids may increase the probability of contamination. Lastly, for better control of spacing, it is necessary to work with low pressures which increase the time to

generate and export drops to glass capillaries. Hence, this method would not work well for time sensitive experiments.

4. Applications of the image-driven drop-on-demand system

We present three diverse applications to demonstrate the capabilities of our system.

4.1. Heterogeneous Belousov–Zhabotinsky droplets

The Belousov–Zhabotinsky (BZ) reaction is the prototypical nonlinear chemical oscillating reaction. It is a metal-ion-catalyzed oscillatory oxidation of the organic substrate, malonic acid, by bromate in an acidic medium, such as sulphuric acid. Previously, we investigated synchronization of coupled identical BZ droplets arranged in linear arrays inside glass capillaries [3]. It was proposed that the coupling is due to the mass transport of two of the BZ chemicals, the inhibitory agent bromine (Br_2) and the activator agent bromine dioxide radical (BrO_2^*), diffusing from drop to drop through intervening oil [2,3,23]. In order to study diffusively coupled oscillators the time scale of diffusion needs to be smaller than the time scale of reaction. For BZ, this requires the reactors to be of the order of 100 μm, which necessitates the use of microfluidics technology.

Here we extend the previous synchronization study to examine coupling between BZ drops of different sizes generated using our drop-on-demand system. The coupling strength was previously predicted to be dependent on drop size [2]. In particular, we predicted that coupling is asymmetric for different sized drops. A small drop can be strongly affected by a large drop, but a large drop is weakly affected by a small drop. Additionally, two small drops are strongly coupled, while two large drops are weakly coupled [2]. Here, we use conditions such that inhibitory coupling is dominant. Specifically, a solution of 300 mM bromate (BrO_3^-), 3 mM ferroin ($Fe(phen)_3^{2+}$), 0.4 mM tris-bipyridine ruthenium ($Ru(bipy)_3^{2+}$), 80 mM sulphuric acid (H_2SO_4), 400 mM malonic acid ($CH_2(COOH)_2$) and 2.5 mM sodium bromide (NaBr) was first prepared and filled in a glass vial. For production of drops, the solution was then fed to one water inlet of the PDMS chip (Fig. 1B.2) while fluorinated oil, HFE-7500, was mixed with 2%v/v of surfactant and fed to the oil inlet using polytetrafluoroethylene (PTFE) capillary tubes. The system was programmed to generate sequences of BZ drops with two different sizes, small drops of 550 pl and large drops of 1100 pl. Drops were then collected and stored in 1D arrays inside cylindrical glass capillaries of 100 μm inner diameter coated with (tridecafluoro-1,1,2,2-tetrahydrooctyl) trichlorosilane to maintain the hydrophobicity. Capillaries containing drops were sealed on microscope slides using epoxy (Hysol® Quick-Cure 5 min epoxy) and images were recorded using a CCD camera mounted on a programmable illumination microscope (PIM) [24] that was also used to optically isolate groups of drops. From video recordings the periods of oscillation between the drop's reduced and oxidized states, were extracted and the phase differences between adjacent drops were calculated.

The dynamical behaviours of linear arrays of drops are shown in Fig. 4. There are 3 drops in the arrays shown in Fig. 4(A.2) and (B.2). The three drops are identical in (A.2) and compared to an array with two small drops and one large drop in (B.2). There are 4 drops in the arrays shown in Fig. 4(C.2) and (D.2). The four drops are identical in (C.2) and compared to an array with three small drops with one large drop in (D.2). Polar plots of the phase difference between drops, shown in the third row of Fig. 4. Drops of the same size always synchronize by locking at a constant phase while, in heterogeneous arrays, the large drop does not synchronize with the rest of the drops in the capillary. Furthermore, control experiments were performed and we found that increasing the drop size by 1/3 speeds up the oscillation by 5% while doubling the light intensity used to set boundaries slows down oscillations of the neighbouring drops by 20%. It was also found that the intrinsic frequency of a drop is independent of the size of boundary drops (see Appendix E). This result demonstrates that the drop-on-demand system can be used to control the coupling strength of chemical oscillations between BZ drops of different size. In a follow-up study we will quantify the strength of drop to drop coupling as a function of drop size mismatch.

4.2. Precipitation of amorphous calcium carbonate in picoliter droplets

Amorphous calcium carbonate (ACC) is a precursor phase to the crystalline polymorphs that form when calcium carbonate is supersaturated [25–27]. In vitro, the ACC to crystal transition is highly unstable and quickly transforms to stable crystalline forms under ambient conditions [25,27–31]. In vivo, controlling the ACC to crystal transition is essential to proper bone and shell development. In previous studies, ACC was produced by encapsulating calcium chloride ($CaCl_2$) solution inside attoliter to femtoliter liposomes, which were immersed in a solution of ammonium carbonate from which carbon dioxide and ammonia diffused into the liposome and initiated precipitation [32]. These studies found that the growth of ACC nanoparticles was controlled by the rate of carbon dioxide and ammonia transport into the calcium-loaded liposomes [25].

Here, we present studies of ACC stability using half nanoliter droplets and demonstrate the utility of the drop-on-demand system for identifying optimal conditions for stabilizing ACC by controlling initial composition, concentration and spacing of drops. With our drop-on-demand system, a sequence of drops containing 1M calcium chloride ($CaCl_2$) alternating with drops containing 0.5M or 0.25M ammonium carbonate ($(NH_4)_2CO_3$) mixed with 1.5M of sodium chloride (NaCl) to reduce the effect of osmotic pressure was generated using fluorinated oil mixed with 2% v/v surfactant and stored as a linear array inside a series of 100 μm diameter cylindrical glass capillaries with separations of 0–100 μm between adjacent drops.

As proposed by a model for biomineralization in confined volumes [25], carbon dioxide and ammonia generated by the ammonium carbonate drop diffuse through the oil into the adjacent calcium chloride drops. This initiates ACC formation in less than 3 min, which is just sufficient time to prepare and position capillaries on the microscope. Subsequently, images were recorded and the growth of the ACC followed by its phase transition to the stable crystal phase were monitored by measuring the intensity of the $CaCl_2$ drops over time. Initially transparent drops became progressively darker as the metastable ACC precipitates. When the ACC transforms into the crystalline phase, the capillary regains transparency as the ACC precipitant, distributed throughout the drop, dissolves and is consumed by the growing crystal via Ostwald ripening, as shown in Fig. 5. With 0.5M of ammonium carbonate, all the drops containing ACC crystallized within 20 min, regardless of the separation distance for 0–100 μm. In contrast, with 0.25M of ammonium carbonate the time to crystallize increased to about 4–5 h for ACC drops in contact with ammonium carbonate drops, while it took 20 days to crystallize 7 of 10 drops, 10 μm far apart, in a sample that was kept sealed at room temperature. Experiments repeated with the same conditions, but done on different days gave similar results.

By controlling the concentration and setting a separation distance drops containing the Ca and CO_2 solutions, we can control the rate of transport of CO_2, which has a profound effect on the longevity of the metastable ACC phase. As a further experiment,

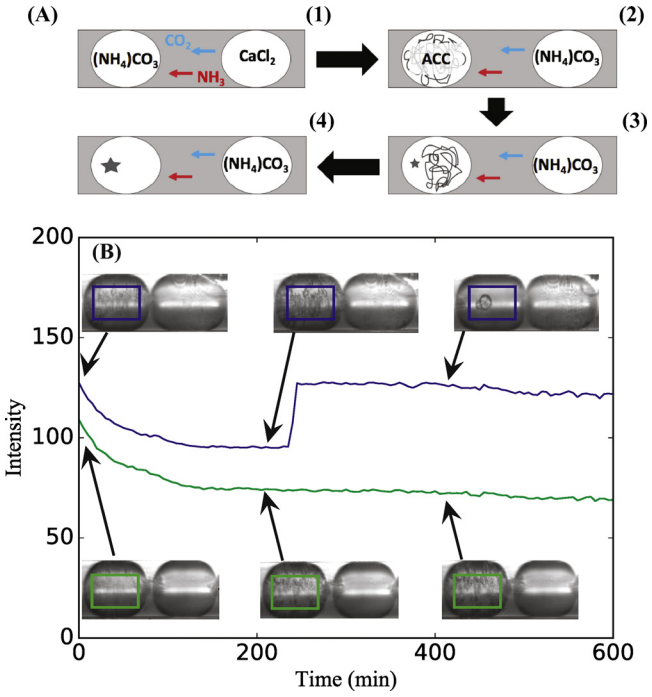

Fig 5. ACC precipitation and crystallization. (A) Schematic illustrating the transport of carbon dioxide (blue) and ammonia (red) through the oil-surfactant mixture interface (grey). (A.1) Initially right drop contains $(NH_4)_2CO_3$, left drop contains $CaCl_2$. The hydration of CO_2 inside the left drop releases protons that lower the drop's pH which leads the NH_4 to disassociate. Both reactions induce (A.2) the precipitation of ACC. (A.3) A crystal nucleates inside the metastable ACC which (A.4) grows into a bigger crystal. (B) Plot of average pixel intensity extracted from regions bounded by rectangles in inset photographs. Each photograph represents a pair of touching (top row, blue) and non-touching (bottom row, green) drops of 1M calcium chloride (left and dark) and 0.25 M ammonium carbonate (right and bright) at instants shown by arrows on the curves. (For interpretation of the references to colour in this figure legend, the reader is referred to the web version of this article.)

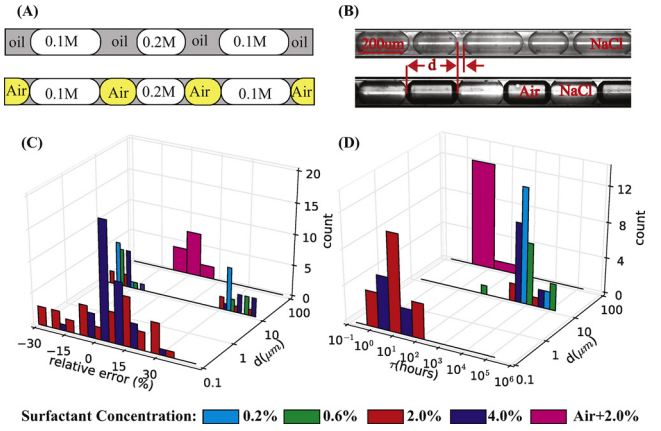

Fig 6. Water exchange between drops containing sodium chloride (NaCl). (A) Schematic illustrating how salt drops (white sphero-cylinders) with different [NaCl] and air bubbles (yellow) are arranged inside glass capillaries filled with oil (grey). (B) Photograph of salt drops (sphero-cylinders) inside cylindrical capillaries separated by (top) oil mixed with surfactant, where initial [NaCl] for small and large drops is 0.2M and 0.1M respectively; and (bottom) air bubbles (darker) separating adjacent drops containing different initial concentrations of salt. d (measured in μm) is the length of the oil gap or air bubble separating two adjacent. (C) The distribution of calculated relative deviations from the expected final concentration $((c - c_{exp})/c_{exp})$ for each drop plotted with respect to d. Since some drops exhibited self-propelling motion, for each drop, d was chosen as the minimum distance to the nearest drop at which it remains static for a period of at least 3 h. (D) The distribution of the time constant necessary for the drop to reach the predicted equilibrium concentration is plotted vs. d. Only drops that remained static for 3 h are considered. (For interpretation of the references to colour in this figure legend, the reader is referred to the web version of this article.)

we propose to measure the rate of transport of CO_2 as function of a fine tuned separation distance between drops.

4.3. Water exchange between drops of sodium chloride

Surfactant molecules play an important role in the compartmentalization process by preventing coalescence and protecting encapsulated materials, such as proteins, from the oil interface. Previous studies done on emulsions of droplets have shown that surfactant micelles can contribute to the transport of materials between droplets [33]. These prior experiments were performed on randomly mixed emulsions containing drops with different concentrations of a hydrophobic dye. It was demonstrated that this dye was transported between drops by micelles. Here, we demonstrate that our image-driven drop-on-demand technology is capable of the study of molecular transport between droplets arranged in a linear capillary as function of both surfactant concentration and distance between droplets. Discrete numbers of droplets of 950 pl and 1300 pl containing 200 mM and 100 mM of sodium chloride (NaCl) respectively were generated sequentially such that neighbouring droplets have different concentrations as shown in Fig. 6A and B. They were separated by distances ranging from 0.1 μm–500 μm and stabilized using HFE-7500 oil mixed with 0.2, 0.6, 2 and 4% of surfactant. Images were then recorded at a frame rate of 1 frame/min for a period of 40 h.

Assuming that no ions are transported through the oil and that the capillaries are well sealed, the initial difference in sodium concentration establishes a chemical potential gradient between drops, which induces diffusion of water molecules from drops with low salt concentration to drops with high salt concentration. Consequently, low concentration drops should shrink while high concentrated drops swell until all drops equilibrate with the same final concentration. Using Fick's laws of diffusion, a model that is described further in Appendix C and D, was used to calculate the instantaneous concentration of a drop given its initial concentration, initial and final volumes. We observed that the exchange of water depended strongly on the size of the oil gap between adjacent drops (see Fig. 6C and D and Appendix F). For experiments run over a period of 40 h, we calculated the deviation from the expected final concentration. It was found that touching drops reached a steady state of concentration with a scatter of about ±15% from the expected concentration within a period of less than 8 h. This large scatter in data may be due to a self-propelling motion observed for some drops [34,35]. During the non-equilibrium process of osmotic transfer of water, some touching drops were observed to spontaneously move apart from each other and thereby increase the separation between drops, which decreased the water exchange rate (see video3 in Appendix). Associated with drop motion, we observed the appearance of small, micron sized globules, which we interpreted as surfactant being desorbed from the drop as it changed size (see video4 in Appendix). When the initial oil gap size was increased to 10–50 μm we found that none of the drops reached a steady state concentration over the course of the experiment. By fitting an exponential function to the change in concentration over time, we found that drops separated by an oil gap of 10–50 μm had an equilibrium constant of about 10^4 h, approximately 1 year. In these experiments, we did not observe any dependence of the surfactant concentration on the water exchange, as opposed to previous work [33] where the exchange of a hydrophobic fluorophore was controlled by micelles produced by the surfactant in the oil.

A further experiment was done in which drops were generated using oil mixed with 2% surfactant. Thereafter, the oil was microflu-

idically drained out and replaced by air bubbles of length about 120–140 μm. All drops were found to reach the equilibrium concentration within a period of 6–9 h. The equilibration rate for drops separated by air is 4 orders of magnitude greater than the one calculated for non-touching drops immersed in oil. This difference is comparable to the ratio of the diffusion coefficient of water in air 0.3 cm^2/s [36] with respect to the diffusion coefficient of water in oil $0.7 \times 10{-}5\ cm^2/s$ [37] at room temperature. In conclusion, there was no evidence that the surfactant micelles mediated exchange of salt, or water, between drops. Drops in oil equilibrate only when they are touching. By separating touching drops by a gap of only a couple of microns, we observed a decrease in exchange rate by four orders of magnitude.

5. Conclusions

The purpose of this drop-on-demand system is to control and measure mass transport on the micron scale by specifying each drop's volume and chemical composition, as well as the inter-drop spacing. To demonstrate the system's versatility, we performed three experiments for aqueous drops in a continuous oil phase. First we investigated synchronization in chemical clocks. Linear arrays of drops containing the Belousov–Zhabontisky (BZ) reaction were constructed containing drops with different sizes. We determined that a large droplet does not synchronize with an array of small drops. However, arrays containing the same number of identical small drops were found to always synchronize. Second, the system was used to vary the stability of the Amorphous Calcium Carbonate (ACC) phase by two orders of magnitude. This was accomplished by altering the distance and chemical concentration between ammonium carbonate drops and calcium chloride drops by small amounts. Third, the drop-on-demand system was used to study water exchange between drops containing sodium chloride as a function of separation and surfactant concentration. The transport rate of water was independent of surfactant concentration and strongly dependent on separation. In two of the three experiments described here, inter-drop distance was the dominant factor controlling the transport rate of materials.

Acknowledgements

We acknowledge support from the Brandeis Center for Bioinspired Soft Materials, and NSF MRSEC, DMR-1420382.

Appendix A. Supplementary data

Supplementary data associated with this article can be found, in the online version, at http://dx.doi.org/10.1016/j.snb.2016.07.065.

References

[1] S.V. Akella, A. Mowitz, M. Heymann, S. Fraden, Emulsion-based technique to measure protein crystal nucleation rates of lysozyme, Cryst. Growth Des. 14 (2014) 4487–4509.
[2] N. Tompkins, N. Li, C. Girabawe, M. Heymann, G.B. Ermentrout, I.R. Epstein, et al., Testing turing's theory of morphogenesis in chemical cells, Proc. Natl. Acad. Sci. U. S. A. 111 (2014) 4397.
[3] J. Delgado, N. Li, M. Leda, H.O. Gonzalez-Ochoa, S. Fraden, I.R. Epstein, Coupled oscillations in a 1D emulsion of Belousov–Zhabotinsky droplets, Soft Matter 7 (2011) 3155–3167.
[4] T.A. Thorsen, Microfluidic tools for high-throughput screening, Biotechniques 36 (2004) 197–199.
[5] J.Q. Boedicker, M.E. Vincent, R.F. Ismagilov, Microfluidic confinement of single cells of bacteria in small volumes initiates high-density behavior of quorum sensing and growth and reveals its variability, Angew. Chem. Int. Ed. 48 (2009) 5908–5911.
[6] P.R. Marcoux, M. Dupoy, R. Mathey, A. Novelli-Rousseau, V. Heran, S. Morales, et al., Micro-confinement of bacteria into w/o emulsion droplets for rapid detection and enumeration, Colloid Surf. A 377 (2011) 54–62.
[7] J.P. Urbanski, W. Thies, C. Rhodes, S. Amarasinghe, T. Thorsen, Digital microfluidics using soft lithography, Lab Chip 6 (2006) 96–104.
[8] Y. Chen, A. Wijaya Gani, S.K. Tang, Characterization of sensitivity and specificity in leaky droplet-based assays, Lab Chip 12 (2012) 5093–5103.
[9] P. Garstecki, M.J. Fuerstman, H.A. Stone, G.M. Whitesides, Formation of droplets and bubbles in a microfluidic T-junction—scaling and mechanism of break-up, Lab Chip 6 (2006) 437–446.
[10] T. Ward, M. Faivre, M. Abkarian, H.A. Stone, Microfluidic flow focusing: drop size and scaling in pressure versus flow-rate-driven pumping, Electrophoresis 26 (2005) 3716–3724.
[11] S.L. Anna, H.C. Mayer, Microscale tipstreaming in a microfluidic flow focusing device, Phys. Fluids 18 (2006).
[12] C.N. Baroud, F. Gallaire, R. Dangla, Dynamics of microfluidic droplets, Lab Chip 10 (2010) 2032–2045.
[13] M.A. Unger, H.P. Chou, T. Thorsen, A. Scherer, S.R. Quake, Monolithic microfabricated valves and pumps by multilayer soft lithography, Science 288 (2000) 113–116.
[14] H.B. Zhou, S.H. Yao, A facile on-demand droplet microfluidic system for lab-on-a-chip applications, Microfluid. Nanofluid. 16 (2014) 667–675.
[15] S.Y. Jung, S.T. Retterer, C.P. Collier, On-demand generation of monodisperse femtolitre droplets by shape-induced shear, Lab Chip 10 (2010) 2688–2694.
[16] J. Xu, D. Attinger, Drop on demand in a microfluidic chip, J. Micromech. Microeng. 18 (2008).
[17] A. Henson, J.M. Gutierrez, T. Hinkley, S. Tsuda, L. Cronin, Towards heterotic computing with droplets in a fully automated droplet-maker platform, Philos. Trans. A Math. Phys. Eng. Sci. 373 (2015).
[18] K. Yamada, T.G. Henares, K. Suzuki, D. Citterio, Paper-based inkjet-printed microfluidic analytical devices, Angew. Chem. Int. Ed. Engl. 54 (2015) 5294–5310.
[19] M.A. Eddings, B.K. Gale, A PDMS-based gas permeation pump for on-chip fluid handling in microfluidic devices, J. Micromech. Microeng. 16 (2006) 2396–2402.
[20] A.C. Rafael, Microfluidic Techniques for the Study of Self-Assembly of Soft Materials [Dissertation], Brandeis University, Waltham, MA, USA, 2014.
[21] C. Holtze, A.C. Rowat, J.J. Agresti, J.B. Hutchison, F.E. Angile, C.H. Schmitz, et al., Biocompatible surfactants for water-in-fluorocarbon emulsions, Lab Chip 8 (2008) 1632–1639.
[22] J. Steigert, S. Haeberle, T. Brenner, C. Muller, C.P. Steinert, P. Koltay, et al., Rapid prototyping of microfluidic chips in COC, J. Micromech. Microeng. 17 (2007) 333–341.
[23] M. Toiya, H.O. Gonzalez-Ochoa, V.K. Vanag, S. Fraden, I.R. Epstein, Synchronization of chemical micro-oscillators, J. Phys. Chem Lett. 1 (2010) 1241–1246.
[24] N. Tompkins, An inexpensive programmable illumination microscope with active feedbac, Am. J. Phys. 84 (2015) 150–158.
[25] C.C. Tester, C.H. Wu, S. Weigand, D. Joester, Precipitation of ACC in liposomes—a model for biomineralization in confined volumes, Faraday Discuss. 159 (2012) 345–356.
[26] C.J. Stephens, Y.Y. Kim, S.D. Evans, F.C. Meldrum, H.K. Christenson, Early stages of crystallization of calcium carbonate revealed in picoliter droplets, J. Am. Chem. Soc. 133 (2011) 5210–5213.
[27] L. Addadi, S. Raz, S. Weiner, Taking advantage of disorder: amorphous calcium carbonate and its roles in biomineralization, Adv. Mater. 15 (2003) 959–970.
[28] S. Weiner, Y. Levi-Kalisman, S. Raz, L. Addadi, Biologically formed amorphous calcium carbonate, Connect. Tissue Res. 44 (2003) 214–218.
[29] C.C. Tester, M.L. Whittaker, D. Joester, Controlling nucleation in giant liposomes, Chem. Commun. 50 (2014) 5619–5622.
[30] F.C. Meldrum, Calcium carbonate in biomineralisation and biomimetic chemistry, Int. Mater. Rev. 48 (2003) 187–224.
[31] J. Aizenberg, S. Weiner, L. Addadi, Coexistence of amorphous and crystalline calcium carbonate in skeletal tissues, Connect. Tissue Res. 44 (Suppl. 1) (2003) 20–25.
[32] C.C. Tester, R.E. Brock, C.H. Wu, M.R. Krejci, S. Weigand, D. Joester, In vitro synthesis and stabilization of amorphous calcium carbonate (ACC) nanoparticles within liposomes, CrystEngComm 13 (2011) 3975–3978.
[33] Y. Skhiri, P. Gruner, B. Semin, Q. Brosseau, D. Pekin, L. Mazutis, et al., Dynamics of molecular transport by surfactants in emulsions, Soft Matter 8 (2012) 10618–10627.
[34] S. Michelin, E. Lauga, D. Bartolo, Spontaneous autophoretic motion of isotropic particles, Phys. Fluids 25 (2013).
[35] T. Toyota, N. Maru, M.M. Hanczyc, T. Ikegami, T. Sugawara, Self-propelled oil droplets consuming fuel surfactant, J. Am. Chem. Soc. 131 (2009) 5012–5013.
[36] E.L. Cussler, Diffusion: Mass Transfer in Fluid Systems, 2nd ed., 1997.
[37] V.K. Vanag, F. Rossi, A. Cherkashin, I.R. Epstein, Cross-diffusion in a water-in-oil microemulsion loaded with malonic acid or ferroin. Taylor dispersion method for four-component systems, J. Phys. Chem. B 112 (2008) 9058–9070.

Biographies

Camille Girabawe is a Ph.D. student in Physics at Brandeis University in Waltham, Massachusetts. He holds a BSc degree in Applied Physics from Kigali Institute of Science and Technology (KIST), Rwanda. He has an interest in microfluidics and synchronization of non-linear chemical oscillators.

Seth Fraden is a professor of physics and director of the Materials Research Science and Engineering Center (MRSEC) at Brandeis University in Waltham, Massachusetts. He completed his BA degree at the University of California, Berkeley and his Ph.D. at Brandeis University. His postdoctoral work was at the Hochfeld Magnet Labor of the Max Planck Institut für Festkorperförschung in Grenoble, France. He received the 2008 Innovation Prize of the International Organization of Biological Crystallization for the development of microfluidic devices for high throughput protein crystallization. Fraden's research focus is experimental Soft Matter; self-assembly in biomaterials, such as liquid crystalline phases of viruses and protein crystallization, and systems far from equilibrium, such as coupled non-linear chemical oscillators.